Diethyl Pyrocarbonate Modification Abolishes Fast Electron Accepting Ability of Cytochrome b_{561} from Ascorbate but Does Not Influence Electron Donation to Monodehydroascorbate Radical: Identification of the Modification Sites by Mass Spectrometric Analysis†

Motonari Tsubaki,*,‡,§ Kazuo Kobayashi,|| Tomoko Ichise,‡ Fusako Takeuchi,‡ and Seiichi Tagawa||

Department of Life Science, Faculty of Science, Himeji Institute of Technology, Kamigoori-cho, Akou-gun, Hyogo 678-1297, Japan, Institute for Molecular Science, Okazaki National Research Institutes, Myodaiji, Okazaki, Aichi 444-8585, Japan, and Institute of Scientific and Industrial Research, Osaka University, Mihogaoka 8-1, Ibaraki, Osaka 567-0047, Japan

Received August 11, 1999; Revised Manuscript Received November 17, 1999

ABSTRACT: Cytochrome b_{561} from bovine adrenal chromaffin vesicles contains two heme B prosthetic groups and transports electron equivalents across the vesicle membranes to convert intravesicular monodehydroascorbate radical to ascorbate. To elucidate the mechanism of the transmembrane electron transfer, effects of the treatment of purified cytochrome b_{561} with diethyl pyrocarbonate, a reagent specific for histidyl residues, were examined. We found that when ascorbate was added to the oxidized form of diethyl pyrocarbonate-treated cytochrome b_{561}, less than half of the heme iron was reduced but with a very slow rate. In contrast, radiolytically generated monodehydroascorbate radical was oxidized rapidly by the reduced form of diethyl pyrocarbonate-modified cytochrome b_{561}, as observed for untreated cytochrome b_{561}. These results indicate that the heme center specific for the electron acceptance from ascorbate was perturbed by the modification of amino acid residues nearby. We identified the major modification sites by mass spectrometry as Lys85, His88, and His161, all of which are fully conserved and located on the extravesicular side of cytochrome b_{561} in the membranes. We suggest that specific *N*-carbethoxylation of the histidyl ligands of the heme *b* at extravesicular side abolishes the electron-accepting ability from ascorbate.

In neurosecretory vesicles, such as adrenomedullary chromaffin vesicles and pituitary neuropeptide secretory vesicles, intravesicular ascorbate (AsA^-)[1] functions as the electron donor for copper-containing monooxygenases such as dopamine β-monooxygenase and peptidyl-glycine α-amidating monooxygenase (*1*, *2*). Upon these monooxygenase reactions, monodehydroascorbate (MDA) radical is produced by univalent oxidation of AsA^- (*3*). It is believed that the intravesicular MDA radical is reduced back to AsA^- by membrane-spanning cytochrome b_{561} and subsequently the oxidized cytochrome b_{561} is reduced by cytosolic AsA^-, since neither AsA^- nor MDA radical can pass through the vesicle membranes (*4*−*6*). Thus, cytochrome b_{561} is likely to serve as an electron conduit, maintaining the AsA^- concentration inside the vesicles for a continuous supply of electron equivalents for the monooxygenase reactions. Indeed, among various cytochromes, cytochrome b_{561} is unique in its localization to neuroendocrine cells in adrenal medulla, gut, pituitary and different regions of brain (*7*, *8*).

Cytochrome b_{561} is a highly hydrophobic hemoprotein (*9*, *10*) with a molecular mass of 29 kDa (*10*) and contains six transmembrane α-helices (*11*, *12*). Recently, we found that purified cytochrome b_{561} contains two hemes *b per* molecule (*13*) and each heme *b* center exhibits a distinct EPR signal in the oxidized state (*13*), consistent with results from an EPR study of oxidized cytochrome b_{561} in chromaffin vesicles (*14*). In addition, very recently, we investigated the reaction of MDA radical with purified cytochrome b_{561} by the technique of pulse radiolysis (*15*). We found that only one of the two heme *b* centers can react with MDA radical (*15*). This finding provides the first clear evidence that the two heme *b* centers have distinct roles for electron donation to MDA radical and electron acceptance from AsA^-, respectively (*15*).

Njus and Kelley (*16*) reported previously that treatment of cytochrome b_{561} in intact chromaffin vesicles with diethyl pyrocarbonate (DEPC), a histidyl imidazole group-specific reagent, inhibited its reduction by external AsA^-, and this inhibition was reversed by hydroxylamine (*16*). On the basis of these observations, they proposed that a histidine residue is involved in the reaction between AsA^- and cytochrome b_{561} (*16*). There are six fully conserved histidyl residues in

† This work was supported by Grant-in-Aids for Scientific Research on Priority Areas (Molecular Biometallics; 10129226 to M.T. and 08249104 to K.K.) and (C) (10680638 to M.T.) from the Japanese Ministry of Education, Science, Sports and Culture.

* Corresponding author: Department of Life Science, Faculty of Science, Himeji Institute of Technology, Kohto 3-2-1, Kamigoori-cho, Akou-gun, Hyogo 678-1297, Japan. Fax 81-791-58-0189; Tel 81-791-58-0189; E-mail tsubaki@sci.himeji-tech.ac.jp.

‡ Himeji Institute of Technology.

§ Okazaki National Research Institutes.

|| Osaka University.

[1] Abbreviations: AsA^-, ascorbate; MDA, monodehydroascorbate; DEPC, diethyl pyrocarbonate; EPR, electron paramagnetic resonance; MALDI-TOF, matrix-assisted laser desorption/ionization time-of-flight.

10.1021/bi991883d CCC: $19.00
Published on Web 03/03/2000

cytochrome b_{561} and four residues among them are possible ligands for two heme *b* prosthetic groups (*17*). Therefore, it is very important to elucidate the inhibition mechanism for understanding of the transmembrane electron-transfer reaction. In the present study, we analyzed the reaction of DEPC with purified cytochrome b_{561}. We found that the DEPC-modified cytochrome b_{561} lost the electron accepting ability from AsA^- but the fast electron donating activity to MDA radical was retained. Further, we identified the DEPC modification sites with matrix-assisted laser desorption/ionization time-of-flight (MALDI-TOF) mass spectrometry.

MATERIALS AND METHODS

Purification of Cytochrome b_{561}. Cytochrome b_{561} was purified to a homogeneous state, as described previously (*13*). The purity of cytochrome b_{561} was analyzed by visible absorption spectra, heme content analysis, and SDS−polyacrylamide gel electrophoresis (*13*). Before use, purified cytochrome b_{561} was concentrated to around 100 μM in an Amicon concentrator with a membrane filter (MWCO = 30 000; Millipore). All other reagents were commercially obtained as the analytical grade. The concentration of cytochrome b_{561} was determined with a millimolar extinction coefficient of 267.9 mM^{-1} cm^{-1} at 427 nm in the reduced state (*13*).

Modification of Cytochrome b_{561} with Diethyl Pyrocarbonate. The concentrated cytochrome b_{561} solution was acidified to pH 6.5 by addition of 0.5 M sodium phosphate buffer (pH 6.0) and was oxidized by stepwise additions of potassium ferricyanide solution (100 mM). Complete oxidation was checked with visible absorption spectroscopy. The oxidized cytochrome b_{561} was gel-filtered through a Sephadex G-25f column equilibrated with 50 mM sodium phosphate buffer (pH 6.5) containing 1.0% (w/v) octyl β-glucoside and was then diluted with the same buffer to an appropriate concentration. The diluted sample was treated with various concentrations of DEPC according to a following procedure.

Optical quartz cells (light path, 1.0 cm) containing 1.0 mL each diluted cytochrome b_{561} solution were placed in sample and reference cell holders of a Shimadzu UV-2200 spectrophotometer. The baseline was recorded before the reaction started. An appropriate amount of DEPC solution (30 mM in dried MeOH) and an equal amount of MeOH were added to the sample and the reference cells, respectively. The spectral changes between 200 and 700 nm were recorded at 2.5 min intervals at room temperature and ceased typically within 30 min.

After cessation of the reaction, the DEPC-treated samples were gel-filtered through a Sephadex G-25f column equilibrated with 50 mM sodium phosphate buffer (pH 6.5) containing 1.0% (w/v) octyl β-glucoside to remove unreacted DEPC. The DEPC-treated cytochrome b_{561} samples were then analyzed for reactivity with AsA^- with a Shimadzu UV-2200 spectrophotometer. Finally, the sample was fully reduced with sodium dithionite and its absorption spectrum was recorded to check the integrity of the heme moiety. The reduction level was analyzed with the absorbance at both 561 (α-band) and 427 nm (Soret band) by normalizing against the level of the dithionite-reduced state.

Pulse Radiolysis. Pulse radiolysis experiments were performed with an electron linear accelerator at the Institute of Scientific and Industrial Research, Osaka University, as previously described (*15, 18, 19*). The pulse width and energy were 8 ns and 27 MeV, respectively. The sample was placed in a quartz cell with an optical path length of 1.0 or 0.30 cm. The temperature of the sample was maintained at 20 °C. A 150 W halogen lamp was used as the light source. After passing through the optical path, the transmitted light intensities were analyzed and monitored by a fast spectrophotometric system composed of a Nikon monochromator, an R-928 photomultiplier, and a Unisoku data analyzing system. Under the condition employed here, the primary radical products [hydrated electron (e_{aq}^-), $OH^\bullet$, and $H^\bullet$] were efficiently converted to MDA radical at an approximate concentration range of 20 μM in the presence of N_2O-saturated 10 mM AsA^-. This concentration could be adjusted by varying the dose of electron beams. The concentration of MDA radical generated by pulse radiolysis was estimated from the absorbance at 360 nm, using a molar extinction coefficient of 3.3 mM^{-1} cm^{-1} (*20*).

Samples of cytochrome b_{561} for pulse radiolysis were prepared as follows. Oxidized cytochrome b_{561} (29 or 178 μM) in 10 mM potassium phosphate buffer (pH 7.0) and 1.0% (w/v) octyl β-glucoside was treated with various concentrations of DEPC (final concentrations 0.05, 0.2, 1.0, and 2.0 mM) for 1 h on ice. Solutions containing 10 mM potassium phosphate buffer (pH 7.0), 1.0% (w/v) octyl β-glucoside, and 10 mM AsA^- were bubbled with N_2O gas for 5 min. Then, untreated or DEPC-treated cytochrome b_{561} were mixed with the AsA^- solution to make a final concentration of cytochrome b_{561} at 5.2 or 89 μM. For each measurement, a fresh sample was used; even though pulse radiolysis did not cause any damage to the sample as judged by its visible absorption spectrum.

Protease Digestion of Cytochrome b_{561}. The digestion was started by addition of protease to oxidized cytochrome b_{561} ($\sim$50 μM) in 50 mM potassium phosphate (pH 6.5) buffer containing 1.0% octyl β-glucoside at room temperature. Final concentrations of the protease used were 0.76 μM for TPCK-treated trypsin (from bovine pancreas; Sigma Chemical Co., St. Louis, MO) and 1.48 μM for V8 protease (from *Staphylococcus aureus* V8; Wako Pure Chemical Industries, Ltd., Osaka, Japan). The extent of the digestion was checked with mass spectrometric analysis at an appropriate interval.

MALDI-TOF Mass Spectrometry. Mass spectrometric analyses were carried out on a Voyager RP mass spectrometer (PerSeptive Biosystems, Farmingham, MA) with 20 kV accelerating voltage. The mass spectra were acquired by adding the individual spectrum from 256 laser shots. For protein analysis the samples were run in a linear mode and for peptide analysis in a reflector mode. The protein solutions were diluted 1:9 (v/v) with a matrix solution, 3,5-dimethoxy-4-hydroxycinnamic acid (Aldrich, Gillingham, England), 50 mg/mL in 30% acetonitrile with 0.3% TFA. The peptide solutions were diluted 1:9 (v/v) with a matrix solution, α-cyano-4-hydroxycinnamic acid (Aldrich, Gillingham, England), 50 mg/mL in 50% acetonitrile with 0.3% TFA. The mixtures (typically 1.0 μL) were deposited on the sample plate and allowed to air-dry before analysis. Insulin (bovine, 5733.69 Da), thioredoxin (*Escherichia coli*, 11 673.68 Da), and apomyoglobin (horse, 16 951.56 Da) were used as external standards for the protein analysis. Angiotensin I (1296.51 Da), ACTH (clip 1−17, 2093.46 Da; clip 18−39,

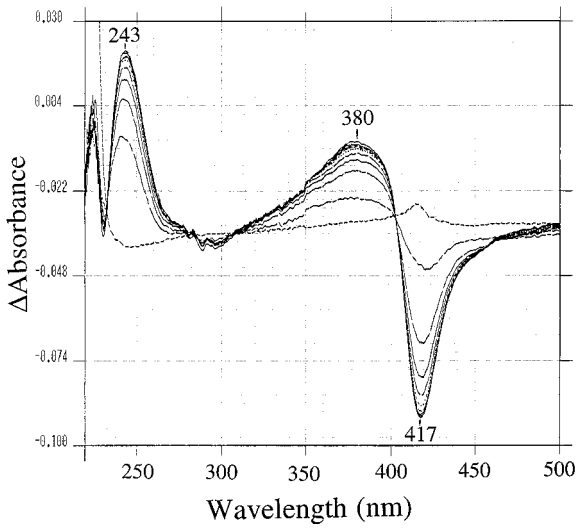

FIGURE 1: Changes in difference spectra upon DEPC treatment of oxidized cytochrome b_{561}. Optical quartz cells (light path, 1.0 cm) containing 1.0 mL each oxidized cytochrome b_{561} [11.2 μM in 1.0% octyl β-glucoside and 50 mM sodium phosphate buffer (pH 6.5)] were placed in sample and reference cell holders of a spectrophotometer. The baseline was recorded before the reaction was started. DEPC (16.7 μL of a 30 mM solution in dried MeOH) and an equal amount of MeOH were added to the sample (final DEPC concentration 0.5 mM) and the reference cells, respectively. The spectral change was recorded at 2.5-min intervals in the region from 500 to 220 nm (taking 1 min and 40 s for each scan) at room temperature.

2465.72 Da; clip 7−38, 3659.19 Da), and insulin (bovine, 5733.69 Da) were used as external standards for the peptide analysis. The positions of the protease cleavage sites in the cytochrome b_{561} amino acid sequence were identified in considering molecular masses of the polypeptide fragments detected by MALDI-TOF mass spectrometry and the specificity of the proteases used. The search of the corresponding fragments in the amino acid sequence of cytochrome b_{561} was carried out using the program GPMAW (v 3.15) (Lighthouse Data, Odense M, Denmark). The molecular masses of all polypeptides measured matched the theoretical ones, obtained from the bovine cytochrome b_{561} amino acid sequence (*11*), within an accuracy of 0.1% or better.

RESULTS

The reaction of DEPC with oxidized cytochrome b_{561} caused spectral changes in both ultraviolet and visible regions as shown in Figure 1. It is well-known that DEPC reacts specifically with an imidazole group of histidyl residues in model systems and in proteins to yield an *N*-carbethoxyhistidyl derivative (*21*). The positive peak at 243 nm in the difference spectrum (Figure 1) is likely due to the formation of an *N*-carbethoxyhistidyl derivative (*21*). Simultaneously, slight spectral changes occurred in the Soret region as a positive peak around 380 nm and a negative peak around 417 nm (Figure 1). The number of modified histidyl residues was calculated from the molar absorption difference for *N*-carbethoxyhistidine ($\Delta\epsilon_{243} = 3.2$ mM^{-1} cm^{-1}) (*21*). It was found to be between 1 and 1.5 *per* cytochrome b_{561} molecule in the concentration ranges from 0.02 to 0.5 mM for DEPC (data not shown) and from 1.37 to 11.2 μM for cytochrome b_{561} (Table 1), respectively. The value of ΔA_{417} upon the DEPC modification was not affected in the concentration range of DEPC from 0.05 to 2.0 mM. Its molar absorption difference ($\Delta\epsilon_{417}$) was estimated to be 6∼8 mM^{-1} cm^{-1} and corresponds to about 3∼4% decrease in absorption of the Soret band of cytochrome b_{561} in the oxidized state (cf. ϵ_{415} = 203.7 mM^{-1} cm^{-1}) (*13*). The spectral changes at 243 and 417 nm occurred with similar time courses as shown in Figure 2. Therefore, it is very likely that the spectral changes in Soret region are due to the secondary perturbation of electronic structure of oxidized heme *b* upon the *N*-carbethoxylation of a few histidyl residues near the heme *b* centers.

Electron-accepting ability from AsA$^-$ was assayed for the DEPC-treated cytochrome b_{561} (Figure 3). In a control experiment, untreated oxidized cytochrome b_{561} was reduced with 2 mM AsA$^-$ very quickly to about 85% reduction level (Figure 3). In contrast, when the DEPC-treated oxidized cytochrome b_{561} was mixed with 2 mM AsA$^-$, less than half of the heme moiety could be reduced in a very slow process (Figures 3 and 4). It took over 10 min to reach a plateau (Figure 3). Similar results were obtained at lower concentrations of the cytochrome (0.7, 2.8, and 5.6 μM; data not shown). Table 1 summarizes numbers of the *N*-carbethoxylated residues and the reduction level after 30 min of incubation with AsA$^-$ at room temperature. These data suggest that the *N*-carbethoxylation of only a few essential histidyl residues caused severe damage to the electron-accepting ability from AsA$^-$. It is important to note, however, that the dithionite-reduced spectra of the control (not shown) and the DEPC-treated samples (Figure 4) were indistinguishable each other.

The electron-transfer activity to MDA radical was examined by the method of pulse radiolysis for the DEPC-treated cytochrome b_{561}. As in the case for the control sample (Figure 5A, upper trace), MDA radical oxidized rapidly the reduced heme *b* center of all the DEPC-treated (0.05−2.0 mM DEPC) cytochrome b_{561} (5.2 μM), as shown in Figure 5B−D. The extent of absorbance change of this process, however, decreased with increasing concentration of DEPC used during the treatment. This result can be explained as due to the decrease of the concentration of the reduced form of cytochrome b_{561} by the DEPC treatment (Table 2). Since a large amount of MDA radical was generated (14.5 μM) under the experimental conditions used for Figure 5, a competition between the disproportionation of MDA radical and the reaction of MDA radical with the reduced form of cytochrome b_{561} might occur. Under this condition, therefore, the reaction of the DEPC-treated samples might be suppressed by the disproportionation of MDA radical. Thus, we conducted a similar experiment but using a much higher concentration (89 μM) of cytochrome b_{561}, with the MDA radical concentration around 1−2.5 μM. The results showed that the DEPC treatment (∼0.05−2.0 mM DEPC) affected neither the apparent rate constant of the absorbance decrease nor the extent of the absorbance change (Figure 6). Indeed, the second-order rate constants for these reactions were found to be around 1.2×10^6 M^{-1} s^{-1} at pH 7.0 and were not affected by the treatment (Table 2). These observations indicate that the DEPC treatment did not cause any appreciable influence on the electron-donating ability to MDA radical. On the other hand, the slower second phase due to the rereduction of the oxidized heme with AsA$^-$ was completely lost upon the treatment (Figures 5B−D and 6B).

Table 1: Effects of the DEPC Treatment of Cytochrome b_{561} on Electron-Accepting Ability from AsA^-

DEPC concn (mM)	cytochrome b_{561} concn (μM)	no. of *N*-carbethoxy-His *per* cytochrome b_{561}[a]	final $\Delta\epsilon_{417}$[a] (mM^{-1} cm^{-1})	reduction with AsA^- (2.0 mM)[b] (%)
0.5	0.70	ND	ND	39.0 (83.5)
0.5	1.37	1.49 ± 0.10	7.23 ± 0.78	35.1 (85.0)
0.5	2.80	1.17 ± 0.09	7.75 ± 0.63	32.1 (83.9)
0.5	11.2	1.34 ± 0.07	6.48 ± 0.60	29.5 (80.8)

[a] Values are the average of three measurements and presented as means ± SD. ND, not determined. [b] Reduction level was calculated on the basis of absorbance at 561 nm. The numbers in parentheses are reduction levels of the corresponding control sample. Values were normalized with dithionite-reduced cytochrome b_{561} as 100%.

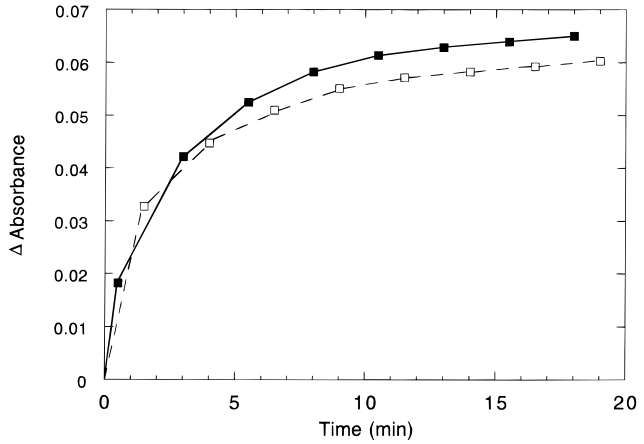

FIGURE 2: Time courses of absorption change at 417 and 243 nm of oxidized cytochrome b_{561} upon DEPC treatment. The absorption changes at 417 (■) and 243 nm (□) for the data in Figure 1 were plotted against time, in considering scanning rate. The absorbance changes at 243 nm were reversed for clarification.

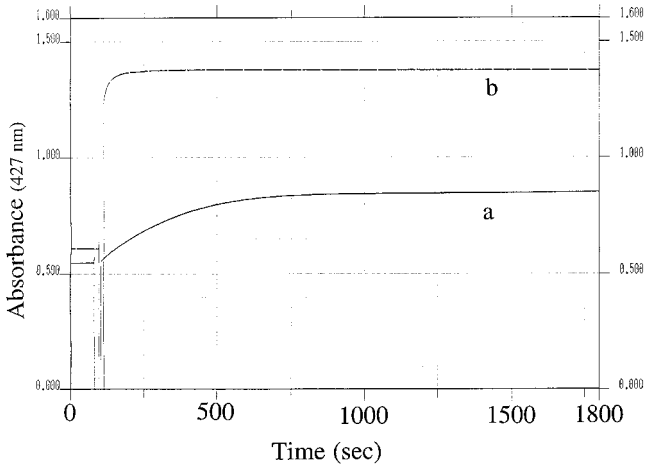

FIGURE 3: Time courses of absorption changes at 427 nm upon reduction with AsA^- of the DEPC-treated (a) and the control (b) samples of oxidized cytochrome b_{561}. An optical quartz cell (light path 1.0 cm) containing 1.0 mL of the control or the DEPC-treated oxidized cytochrome b_{561} [11.2 μM in 1.0% octyl β-glucoside and 50 mM sodium phosphate buffer (pH 6.5)] was placed in a spectrophotometer. Twenty milliliters of AsA^- solution (100 mM in the buffer) was added (final concentration 2.0 mM) and the absorption change at 427 nm was recorded in the time-scan mode at room temperature for 30 min.

DEPC is also known to react with a variety of nucleophilic residues including sulfhydryl, arginyl, lysyl, and tyrosyl residues in model reactions (*21*). It is reported that *O*-carbethoxylation of *N*-acetyl-L-tyrosine ethyl ester results in a difference spectrum that shows a minimum at 278 nm ($\Delta\epsilon_{278}$ = 1.31 mM^{-1} cm^{-1}) and a major decrease at

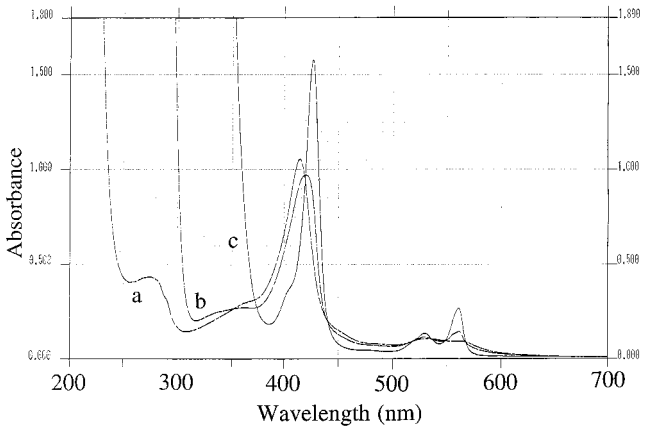

FIGURE 4: Visible absorption spectra of the DEPC-treated cytochrome b_{561} in oxidized (a), AsA^--reduced (b), and dithionite-reduced (c) states. The DEPC- (0.5 mM) treated cytochrome b_{561} (11.2 μM in oxidized state) was gel-filtered against 1.0% octyl β-glucoside and 50 mM sodium-phosphate buffer (pH 6.5). The visible absorption spectrum was recorded. Then, AsA^- was added (final 2.0 mM) and incubated for 30 min at room temperature and the visible spectrum was recorded. Finally, sodium dithionite was added and the visible spectrum was recorded.

wavelengths below 240 nm (*21*). However, we did not observe significant spectral change in this region for any of the DEPC concentrations used. It is reported that the *N*-carbethoxylation of imidazole group can be reversed by treatment of hydroxylamine (*21*). Although we tried to restore the DEPC modification with hydroxylamine for the early stage of our study, the recovery (including the electron-transfer activity) was not complete and its extent was not reproducible. This suggests that amino acid residues other than histidyl (or tyrosyl) residues may also be modified upon DEPC treatment (*21*). To clarify the sites of the DEPC modification, we carried out MALDI-TOF mass spectrometric analyses.

The mass spectrum of intact cytochrome b_{561} in oxidized state in the presence of 1.0% octyl β-glucoside was directly analyzed in a linear mode. The spectrum showed a clear ($M + H^+$) peak at 28 030 *m*/*z* (Figure 7A). This value is slightly higher than the theoretical value of 27 901.9 based on the deduced amino acid sequence (*11*). This result is consistent with the report that the NH_2-terminus of cytochrome b_{561} was blocked by an unknown modification(s) (*10*, *11*). The DEPC (0.5 mM) treatment of oxidized cytochrome b_{561} caused a slight mass shift to 28 250 *m*/*z* (Figure 7B), suggesting that about three carbethoxy groups (73.0 Da × 3) *per* one molecule of cytochrome b_{561} were introduced. This observation is consistent with our suggestion that an additional DEPC modification site (or sites) exists other than the two histidyl residues.

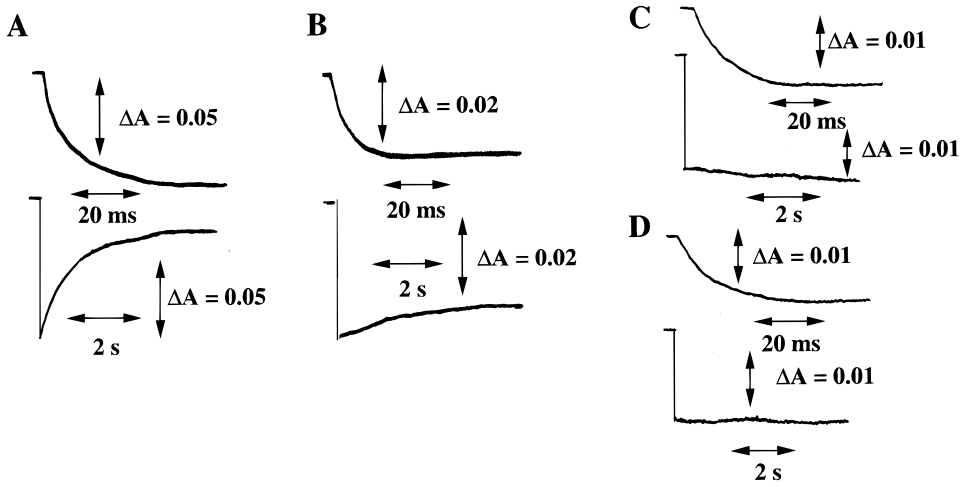

FIGURE 5: Reactions with MDA radical of the control (A) and the DEPC-treated [0.05 mM (B), 0.20 mM (C), and 1.0 mM (D)] samples of cytochrome b_{561} in the reduced state and following slow reactions with AsA^- of the corresponding samples in the oxidized state after pulse radiolysis. The reaction mixture contained 5.2 μM cytochrome b_{561}, 5 mM AsA^-, 1.0% octyl β-glucoside, and 10 mM potassium phosphate buffer (pH 7.0). The absorption changes were monitored at 430 nm for both fast (upper trace) and slow (lower trace) phases at room temperature.

Table 2: Effects of DEPC Treatment of Oxidized Cytochrome b_{561} on Second-Order Rate Constants for the Electron Donation and Acceptance from MDA Radical and AsA^-, Respectively[a]

DEPC concn (mM)	reduced with AsA^- (5.0 mM)[b] (%)	rate constant for oxidation with MDA radical[c] (M^{-1} s^{-1})	rate constant for reduction with AsA^- (M^{-1} s^{-1})
control	85	1.2×10^6	4.8×10^2
0.05	64	1.3×10^6	none
0.20	48	1.2×10^6	none
1.0	33	1.3×10^6	none
2.0	28	1.8×10^6	none

[a] Cytochrome b_{561} concentrations were 29 μM (for DEPC treatment) or 14.5 μM (for pulse radiolysis) in 10 mM potassium phosphate buffer (pH 7.0) and 1.0% octyl β-glucoside. [b] Reduction level was calculated on the basis of absorbance at 561 nm. Normalized with dithionite-reduced cytochrome b_{561} as 100%. [c] Normalized with the concentration of the reduced form of cytochrome b_{561}.

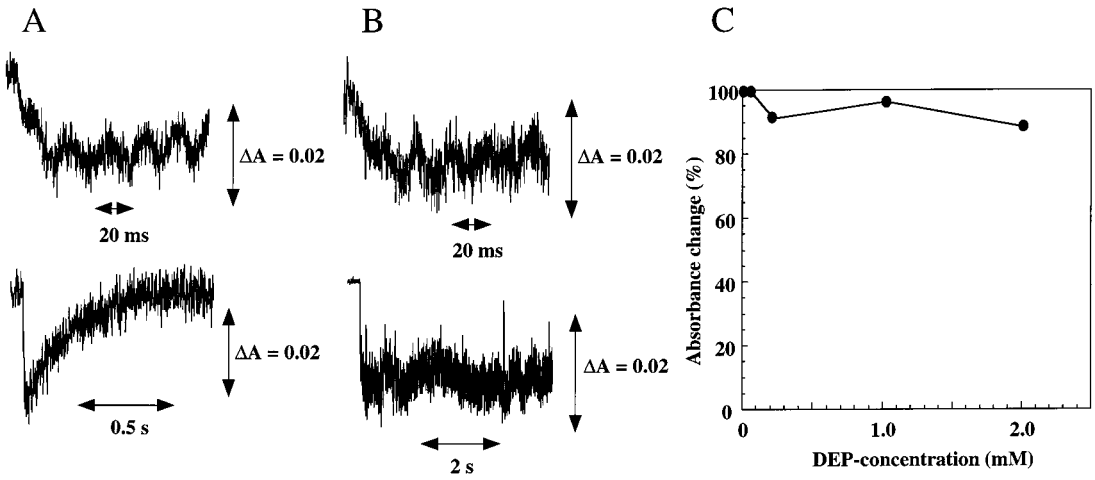

FIGURE 6: Reactions with MDA radical of the control (A) and the DEPC- (1.0 mM) treated (B) samples at higher concentration of cytochrome b_{561} in reduced state, following reactions with AsA^- of the corresponding samples in oxidized state after pulse radiolysis, and the effect of the DEPC concentration on the extent of the absorbance change in electron donation to MDA radical (C). The reaction mixture contained 89 μM cytochrome b_{561}, 5 mM AsA^-, 1.0% octyl β-glucoside, and 10 mM potassium phosphate buffer (pH 7.0). The absorption changes were monitored at 561 nm for both the faster (upper trace) and the slower (lower trace) phases at room temperature. In panel C, the extent of the absorbance change for the control sample was taken as 100%.

MALDI-TOF mass spectrometric analyses of a tryptic digest from untreated cytochrome b_{561} showed many partially cleaved polypeptides (Figure 8A). Careful analyses identified most of these polypeptides unambiguously, as indicated. The assignment covers about 92% of the deduced amino acid sequence. Only NH_2-terminal and COOH-terminal tryptic peptides were not identified (Table 3). Mass analyses of a tryptic digest from the DEPC-treated cytochrome b_{561} identified several singly, doubly, and triply modified polypeptides as indicated by mass shifts of +72, +144, and +216 (m/z), respectively (Figure 8B), suggesting that multiple carbethoxylation occurs. In addition, there were many polypeptides

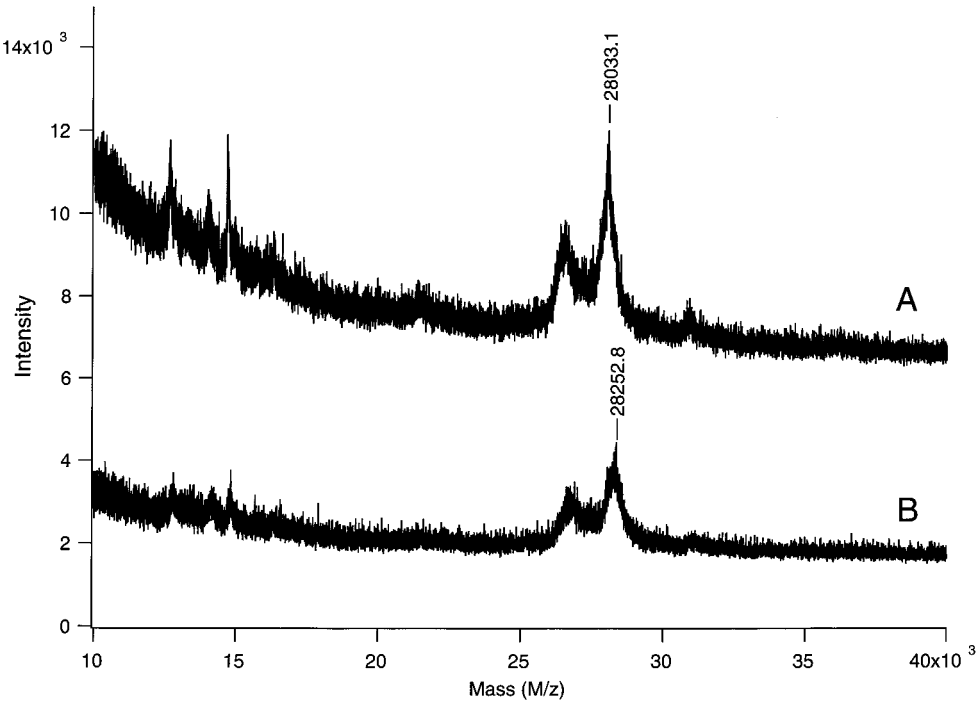

FIGURE 7: MALDI-TOF mass spectra of cytochrome b_{561} before (a) and after (b) DEPC treatment. Mass spectra were obtained as described in the text. The peak around 26 500 (*m*/*z*) is probably due to a partially cleaved form of cytochrome b_{561}.

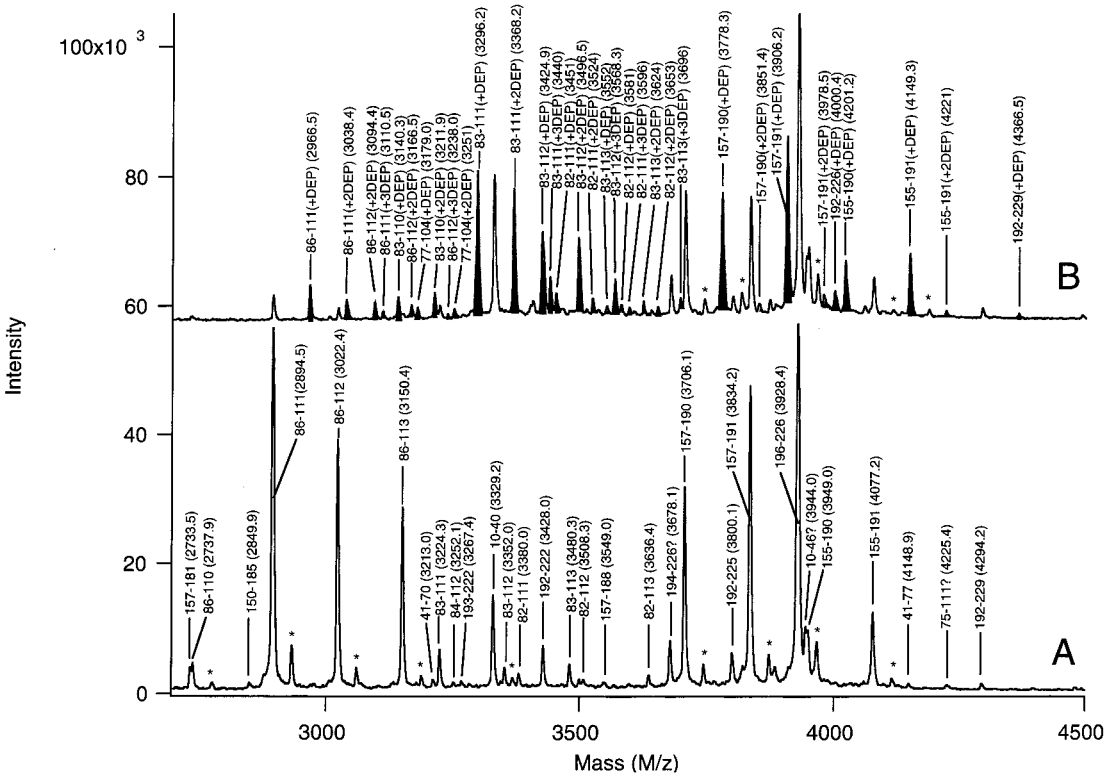

FIGURE 8: MALDI-TOF mass spectra of tryptic digests obtained from untreated (A) and DEPC treated (B) cytochrome b_{561}. Tryptic digests were obtained as described in the text. A mixture of the polypeptides was directly analyzed with MALDI-TOF mass spectrometry. Other conditions are described in the text. The number for each peak indicates the assignment of each polypeptide by a range of amino acid residues. The peaks corresponding to polypeptides containing carbethoxy groups are shaded, and the number of carbethoxy groups introduced into the polypeptide is indicated (e.g., +2DEP). The number in the parentheses indicates the observed mass value (*m*/*z*) for each peak. Peaks indicated by an asterisk are due to $[M + K^+]$ species.

exhibiting much larger shifts, which could not be explained by the usual *N*-carbethoxylation of histidyl residues. Careful analyses of the masses of these unusual polypeptides revealed that one lysyl residue (Lys85) is selectively *N*-carbethoxylated upon DEPC treatment, resulting in a noncleavable site upon the tryptic digestion. We could assign most of these carbethoxylated tryptic peptides, as indicated in Figure 8B. In considering the nucleophilicity of amino acid residues,

Table 3: Tryptic Peptides Based on the Deduced Amino Acid Sequence of Bovine Cytochrome b_{561}

no.	residues	avg mass	sequence
1	1−9	915.04	MEGPASPAR
2	10−40	3330.02	APGALPYYVAFSQLLGLIVVAMTGAWLGMYR
3	41−74	3744.46	GGIAWESALQFNVHPLCMIIGLVFLQGDALLVYR
4	75−77	420.51	VFR
5	78−81	460.49	NEAK
6	82−82	174.20	R
7	83−85	348.40	TT**K**
8	86−111	2894.50	VL**H**GLL**H**VFAFVIALVGLVAVFEHHR
9	112−112	146.19	K
10	113−113	146.19	K
11	114−154	4681.46	GYADLYSLHSWCGILVFALFFAQWLVGFSFFLFPGASFSLR
12	155−156	261.28	SR
13	157−181	2733.30	YRPQ**H**VFFGAAIFLLSVATALLGLK
14	182−191	1120.31	EALLF**E**LGTK
15	192−222	3429.12	**Y**SMFEPEGVLANVLGLLLATFATVIL**Y**ILTR
16	223−226	518.57	ADWK
17	227−241	1763.00	RPLQAEEQALSMDFK
18	242−252	1121.12	TLTEGDSPSSQ

[a] The DEPC modification sites are indicated in boldface type, and three major sites among them are underlined.

possible modification sites, in addition to Lys85, could be listed as follows. (1) One major and one minor sites in tryptic peptide 86−111 (possible sites His88, His92, His109, and His110). (2) One major and one minor sites in tryptic peptide 157−191 (possible sites Tyr157, Arg158, His161, and Lys181). (3) Two minor sites in tryptic peptide 192−222 (possible sites Tyr192 and Tyr218). Prolonged incubation with trypsin resulted in a further digestion of the tryptic peptides into shorter polypeptides, possibly due to contaminating chymotrypsin or other unknown protease activities. A part of these polypeptides showed a mass shift by +72 or +144 (*m*/*z*) for the DEPC-treated sample. These include polypeptide 84−101 [+144 (*m*/*z*)], polypeptide 87−103 [+72 (*m*/*z*)], and polypeptide 160−181 [+72 (*m*/*z*)] (spectra not shown).

To identify the DEPC modification sites more specifically, mass analyses of V8 peptides from untreated and DEPC-treated cytochrome b_{561} were performed similarly. The assignment covered almost the whole sequence except for several residues in the NH_2-terminal portion (spectra not shown for the analyses of V8 peptides). Two V8 peptides, 3−46 and 47−79, did not show any indication of DEPC modification. Two V8 peptides, 188−233 and 191−233, showed two minor DEPC modification sites, respectively, whereas a shorter V8 peptide, 199−233, carries only one DEPC modification site. Although the middle part of cytochrome b_{561} did not give V8 peptides in significant amounts in the mass spectra, there were several peaks of weak intensity derived from this part. V8 peptide 80−108 showed two major modification sites, whereas V8 peptide 109−187 showed one major and one minor modification site. Prolonged incubation with V8 protease at room temperature resulted in cleavages other than the authentic cleavage sites, leading to formation of shorter polypeptides. Some of these polypeptides showed a mass shift of +144 (*m*/*z*), indicating presence of two DEPC modification sites. These are polypeptides 68−126, 43−95, and 73−95.

Considering all these mass spectrometric data, we conclude that there are three major DEPC modification sites at Lys85, His161, and His88 (or His92) for oxidized cytochrome b_{561}. Additional three minor modification sites[2] are, possibly, at His92 (or His88), Tyr218, and Tyr192, the latter being the least modified site.

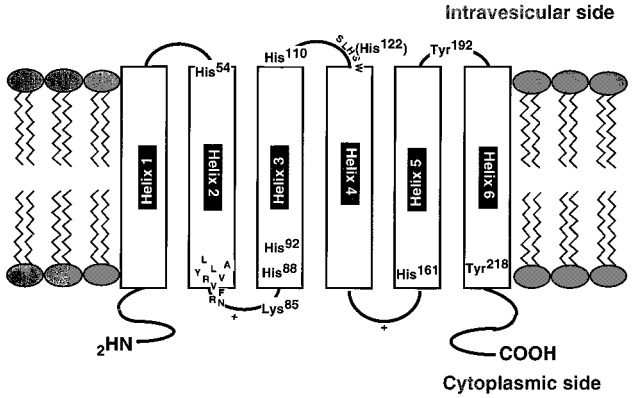

FIGURE 9: Plausible model of transmembrane structure of cytochrome b_{561}. Two fully conserved sequences and 6 histidyl residues (which include two major DEPC modification sites) are indicated, in addition to other DEPC modification sites (Lys85, Tyr192, and Tyr218).

DISCUSSION

In a series of our recent studies, we have revealed the following fundamental properties of cytochrome b_{561}, on which our present study stands. First, EPR spectra of purified cytochrome b_{561} in the oxidized state showed two distinct heme *b* species (*13*). One species showed a usual low spin signal ($g_z = 3.14$), and the other gave a highly anisotropic low-spin signal ($g_z = 3.70$) (*13*). It is likely that the heme *b* center with a lower redox potential (the $g_z = 3.70$ species) is participating in electron acceptance from extravesicular AsA^-, and the other ($g_z = 3.14$) with a higher redox potential is responsible for the electron donation to MDA radical (*13*). Second, we have proposed a plausible structural model of cytochrome b_{561} on the basis of comparison of the deduced amino acid sequences of seven species (*17*). In the proposed model (Figure 9), there are two fully conserved regions in the sequences; the first one (^{69}ALLVYRVFR^{77}) is located on the extravesicular side of an α-helical segment, and the

[2] The fourth minor modification site, residing in tryptic peptide 157−191, could not be identified in the present study.

second one (^{120}SLHSW^{124}) is located in an intravesicular loop connecting two α-helical segments (*17*). These conserved sequences are likely to form the binding sites for extravesicular AsA^- and intravesicular MDA radical, respectively, and the two heme *b* centers may be located on each side of the vesicular membranes in close contact with these sites, respectively (*17*). Third, a pulse radiolysis study showed that one of the heme *b* centers in cytochrome b_{561} specifically reacts with MDA radical, whereas the other does not (*15*). This was verified by the experiment of MDA radical concentration dependence on the oxidization of cytochrome b_{561} after pulse radiolysis. The pH dependence of the rate constants of the two electron-transfer reactions provided further implication for the function of cytochrome b_{561}. The optimal pH of the oxidation (pH 5.5) and the reduction (pH 6.8) of the heme centers were found to correspond to physiological pH at the intravesicular and extravesicular sides, respectively (*15*). On the other hand, when the reactions were examined for cytochrome b_{561} pretreated in a mild alkaline condition in oxidized state (*17*), the reduced form of cytochrome b_{561} could not be oxidized with MDA radical. This result suggests that the heme center for the electron donation to MDA radical is selectively modified upon the alkaline treatment (*15*).

In the present study, we found that the DEPC treatment of cytochrome b_{561} in oxidized state selectively destroyed the fast electron-accepting ability from AsA^-. However, the fast electron-donating activity to MDA radical was retained. MALDI-TOF mass spectrometric analyses identified three major DEPC modification sites, i.e., two histidyl [His161 and His88 (or His92)] residues and one lysyl (Lys85) residue, in addition to three minor modification sites. Although we could not assign unambiguously which of two histidyl residues (His88 and His92) was the major modification site, we consider that His88 is much more likely. This is based on the following reasons. (1) According to the structural model (Figure 9), His92 must be located deeply inside the molecule, in which the access of DEPC will be restricted. (2) His92 turned out to be not a conserved residue upon analysis of planarian cytochrome b_{561} cDNA (Asada et al., unpublished result) and, therefore, not a heme ligand. Thus, imidazole groups of His161 and His88, which are considered as ligands for the heme *b* located on the extravesicular side (Figure 9), are selectively modified with DEPC. The observation that the development of the 243-nm band ascribable to *N*-carbethoxyhistidyl derivatives was accompanied by concomitant spectral changes around Soret region in the difference spectrum (Figures 1 and 2) is consistent with our proposal. However, it must be mentioned that the dithionite-reduced spectra of the control and the DEPC-treated samples were indistinguishable from each other. This fact suggests that the *N*-carbethoxylation occurred at the noncoordinating nitrogen atom of the imidazole groups and did not cause any drastic structural damage around the heme *b* moiety (such as breakage of the heme iron−imidazole coordination, as observed for myoglobin and cytochrome b_5) (*22*).

It is reported that purified cytochrome b_{561} gave two midpoint potentials, at +170 and +70 mV (*23*). Considering the midpoint potential of AsA^-/MDA couple (+330 mV at pH 7.0) (*16*), the inhibition mechanism can be most easily explained as a drastic change of midpoint potential of the heme *b* on the extravesicular side. The *N*-carbethoxylation of the heme-coordinating imidazole ring might cause a drastic lowering of the ligand field strength because of the electron-withdrawing ability of the carbethoxy group. The slight but clear spectral changes of the Soret band in the oxidized state may be a reflection of the lowering. This may lead to a considerable decrease of the midpoint potential of the heme *b* on the extravesicular side, which can no longer accept electrons from AsA^-. Alternatively, the presence of an *N*-carbethoxy group at the heme-coordinating imidazole ring may inhibit the access of AsA^- to the specific binding site for the electron donation (see later discussion).

For the DEPC-treated cytochrome b_{561} sample, about 30% of the oxidized heme could be reduced by AsA^- but with a very slow rate. The slow reduction process is likely an electron backflow from AsA^- to the oxidized heme *b* at the intravesicular side, which is normally responsible for the electron donation to MDA radical. A reversed electron flow further to the oxidized heme *b* on the extravesicular side, which is responsible for electron acceptance from AsA^-, cannot occur for the DEPC-treated cytochrome b_{561}. Njus and co-workers, however, showed that a completely reversed electron flow could occur in chromaffin vesicles (*4, 24*). An AsA^--loaded chromaffin vesicle ghost could donate electrons to extravesicular cytochrome *c* or ferricyanide via membrane-spanning cytochrome b_{561} (*4, 24*), although its rate was very slow. They proposed that the rate of the reversed electron transfer through cytochrome b_{561} is limited by the rate at which cytochrome b_{561} is reduced by intravesicular AsA^-, since the cytochrome b_{561} heme is nearly completely oxidized during the transmembrane electron transfer (*24*).

It is noteworthy that all the DEPC modification sites, except for Tyr192, seem to be distributed in a very narrow region facing the extravesicular side when we imagine the three-dimensional structure of cytochrome b_{561} in the membranes (Figure 9). The role of Lys85 for the electron-transfer reaction from AsA^- is not clear. However, since this residue is fully conserved and located at the extravesicular surface of the molecule (Figure 9), it is likely that this positively charged group has a role in the recognition of AsA^-, in conjunction with other well-conserved positively charged residues and the fully conserved sequence (^{69}ALLVYRVFR^{77}). The selective DEPC modification of Lys85 residue among many lysyl and arginyl residues (total 19) may be related to the existence of such a specific binding site near the heme *b* center. The modification of tyrosyl residues with DEPC was not significant, as expected from the absence of spectral change around 278 nm (Figure 1). Tyr218, a minor modification site with DEPC, also is located on the extravesicular side of the molecule (Figure 9). The role of this residue is also not clear at this stage. Since this residue is fully conserved for vertebrate cytochrome b_{561} (*17*), a possible role for electron transfer between two heme *b* centers may be suggested. Tyr192, the least modified site, is located in an intravesicular loop (Figure 9). This residue is also highly conserved (*17*). To elucidate the precise role of these conservative residues, further studies are in progress.

Now, the mechanism of inhibition of the transmembrane electron transfer upon DEPC treatment, first reported by Njus and Kelley (*16*), can be easily understood on the basis of our present study. We suggest that the specific *N*-carbethoxylation of histidyl ligands (His88 and His161) of the

heme *b* on the extravesicular side abolishes the electron-accepting ability from AsA^-. Present results, in conjunction with our previous observations, lead to a firm conclusion that the two heme *b* centers of cytochrome b_{561} have distinct roles for electron donation to MDA radical and electron acceptance from AsA^-, respectively.

ACKNOWLEDGMENT

We thank the members of the Radiation Laboratory in the Institute of Scientific and Industrial Research, Osaka University, for assistance in operating the accelerator.

REFERENCES

1. Eipper, B. A., Mains, R. E., and Glembotski, C. C. (1983) *Proc. Natl. Acad. Sci. U.S.A. 80*, 5144−5148.
2. Kent, U. M., and Fleming, P. J. (1987) *J. Biol. Chem. 262*, 8174−8178.
3. Dhariwal, K. R., Black, C. D. V., and Lavine, M. (1991) *J. Biol. Chem. 266*, 12908−12914.
4. Njus, D., Knoth, J., Cook, C., and Kelley, P. M. (1983) *J. Biol. Chem. 258*, 27−30.
5. Njus, D., Kelley, P. M., and Harnadek, G. J. (1986) *Biochim. Biophys. Acta 853*, 237−265.
6. Wakefield, L. M., Cass, A. E. G., and Radda, G. K. (1986) *J. Biol. Chem. 261*, 9739−9745.
7. Duong, L. T., Fleming, P. J., and Russell, J. T. (1984) *J. Biol. Chem. 259*, 4885−4889.
8. Pruss, R. M., and Shepard, E. A. (1987) *Neuroscience 22*, 149−157.
9. Silsand, T., and Flatmark, T. (1974) *Biochim. Biophys. Acta 359*, 257−266.
10. Duong, L. T., and Fleming, P. J. (1982) *J. Biol. Chem. 257*, 8561−8564.
11. Perin, M. S., Fried, V. A., Slaughter, C. A., and Südhof, T. C. (1988) *EMBO J. 7*, 2697−2703.
12. Kent, U. M., and Fleming, P. J. (1990) *J. Biol. Chem. 265*, 16422−16427.
13. Tsubaki, M., Nakayama, M., Okuyama, E., Ichikawa, Y., and Hori, H. (1997) *J. Biol. Chem. 272*, 23206−23210.
14. Burbaev, D. S., Moroz, I. A., Kamensky, Y. A., and Konstantinov, A. A. (1991) *FEBS Lett. 283*, 97−99.
15. Kobayashi, K., Tsubaki, M., and Tagawa, S. (1998) *J. Biol. Chem. 273*, 16038−16042.
16. Njus, D., and Kelley, P. M. (1993) *Biochim. Biophys. Acta 1144*, 235−248.
17. Okuyama, E., Yamamoto, R., Ichikawa, Y., and Tsubaki, M. (1998) *Biochim. Biophys. Acta 1383*, 269−278.
18. Kobayashi, K., Harada, Y., and Hayashi, K. (1991) *Biochemistry 30*, 8310−8315.
19. Kobayashi, K., Tagawa, S., Sano, S., and Asada, K. (1995) *J. Biol. Chem. 270*, 27551−27554.
20. Cabelli, D. E., and Bielski, B. H. J. (1983) *J. Phys. Chem. 87*, 1809−1812.
21. Miles, E. W. (1977) *Methods Enzymol. 47*, 431−442.
22. Konopka, K., and Waskell, L. (1988) *Biochim. Biophys. Acta 954*, 189−200.
23. Apps, D. K., Boisclair, M. D., Gavine, F. S., and Pettigrew, G. W. (1984) *Biochim. Biophys. Acta 764*, 8−16.
24. Kelley, P. M., and Njus, D. (1986) *J. Biol. Chem. 261*, 6429−6432.

BI991883D